Realization of Practical Eightfold Fermions and Fourfold van Hove Singularity in $TaCo_2Te_2$

Hongtao Rong[1#], Zhenqiao Huang[1,7#], Xin Zhang[2,8#], Shiv Kumar[3#], Fayuang Zhang[1], Chengcheng Zhang[1], Yuan Wang[1], Zhanyang Hao[1], Yongqing Cai[1], Le Wang[1], Cai Liu[1], Xiao-Ming Ma[1], Shu Guo[1], Bing Shen[4], Yi Liu[5], Shengtao Cui[5], Kenya Shimada[3], Quansheng Wu[6,10], Junhao Lin[1], Yugui Yao[2,8], Zhiwei Wang[2,8,9*], Hu Xu[1*], and Chaoyu Chen[1*]

[1] Shenzhen Institute for Quantum Science and Engineering (SIQSE) and Department of Physics, Southern University of Science and Technology (SUSTech), Shenzhen 518055, China.

[2] Centre for Quantum Physics, Key Laboratory of Advanced Optoelectronic Quantum Architecture and Measurement, School of Physics, Beijing Institute of Technology, Beijing 100081, China.

[3] Hiroshima Synchrotron Radiation Centre, Hiroshima University, Higashi-Hiroshima, Hiroshima 739-0046, Japan.

[4] School of Physics, Sun Yat-Sen University, Guangzhou 510275, China.

[5] National Synchrotron Radiation Laboratory, University of Science and Technology of China, Hefei, Anhui 230029, China.

[6] Beijing National Laboratory for Condensed Matter Physics, and Institute of Physics, Chinese Academy of Sciences, Beijing 100190, China.

[7] Department of Physics, The Hong Kong University of Science and Technology, Clear Water Bay, Hong Kong, China.

[8] Beijing Key Lab of Nanophotonics and Ultrafifine Optoelectronic Systems, Beijing Institute of Technology, Beijing 100081, China.

[9] Material Science Center, Yangtze Delta Region Academy of Beijing Institute of Technology, Jiaxing 314011, China.

[10] University of Chinese Academy of Sciences, Beijing 100049, China.

[#] These authors contributed equally to this work.

[*]Correspondence should be addressed to Z.W. (zhiweiwang@bit.edu.cn), H.X. (xuh@sustech.edu.cn) and C.C. (chency@sustech.edu.cn)

Supplementary Materials

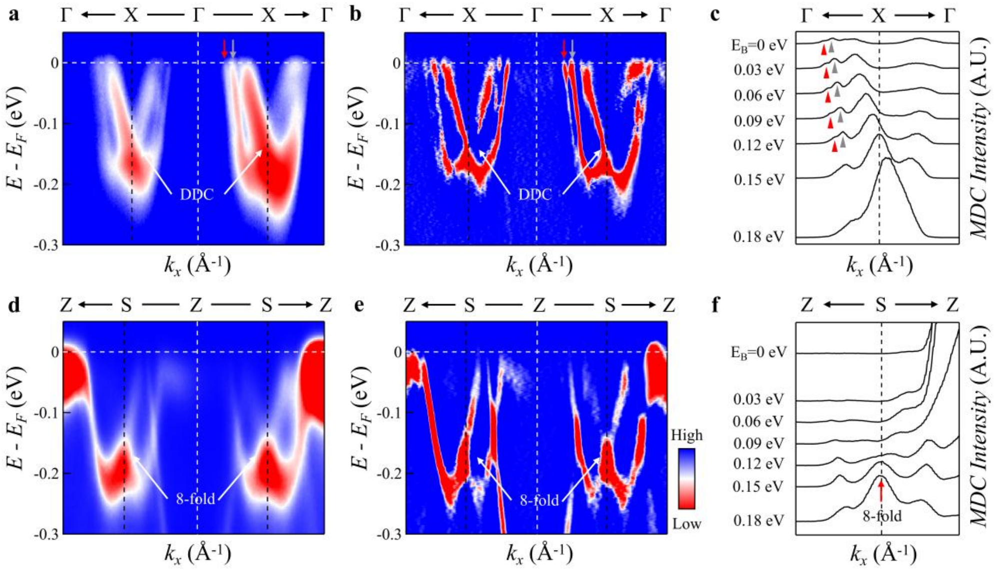

Supplementary Figure 1. Double Dirac cone feature and eightfold fermion in $TaCo_2Te_2$. (a-c) Double Dirac cone spectral feature in $TaCo_2Te_2$. ARPES intensity plot (a) and second derivative plot of (a) along the $\Gamma - X - \Gamma - X - \Gamma$ direction. (c) Momentum distribution curve plots along the $\Gamma - X - \Gamma$ direction. In supplementary Fig. S1 (b) and (c), red arrows and gray arrows indicate the band splitting. ARPES intensity plot (d) and second derivative plot of (e) along the $Z - S - Z - S - Z$ direction. (c) Momentum distribution curve plots along the $Z - S - Z$ direction. Red arrow indicates eightfold fermion in supplementary Fig. 1(f).

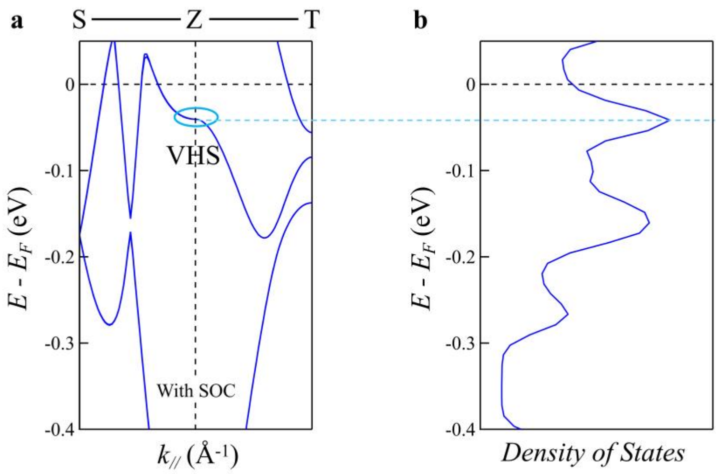

Supplementary Figure 2. DFT calculated the band structure (a) and density of states (b) of $TaCo_2Te_2$ along the $S - Z - T$ direction. (a) DFT calculated the band structure along $S - Z - T$ direction which shows the fourfold van Hove singularity at Z point. (b) the corresponding density of states of supplementary Fig. 2(a). It shows the density of states at the fourfold van Hove singularity is obviously enhanced.

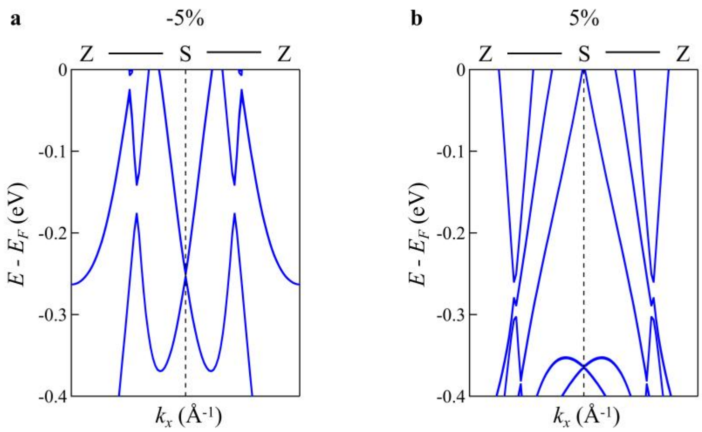

Supplementary Figure 3. The band structure of $TaCo_2Te_2$ under (a) -5% and (b) 5% uniaxial strain along [100] direction. The gap at S point is almost unchanged since the strain in this direction will not change the symmetry of the system.

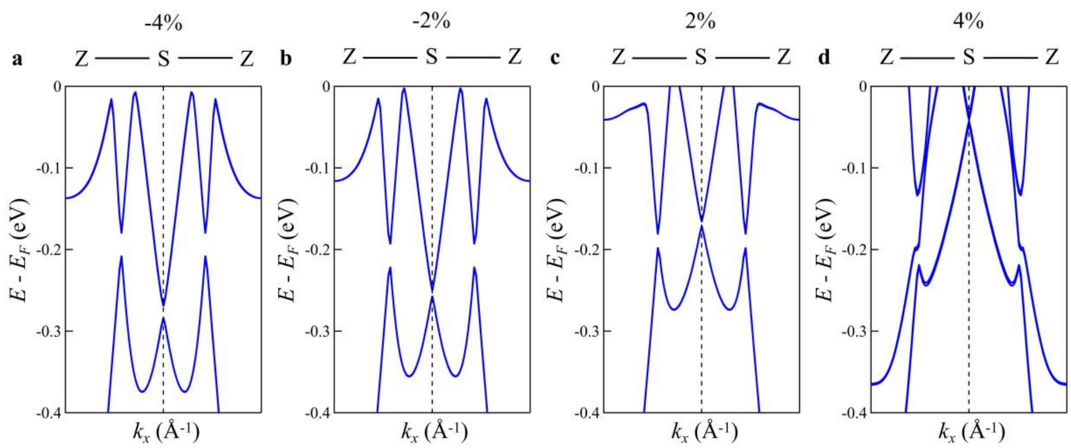

Supplementary Figure 4. The band structure of $TaCo_2Te_2$ under (a) -4%, (b) -2%, (c) 2% and (d) 4% uniaxial strain along [110] direction. The strain will break the symmetry to open a gap and move the practical eightfold crossing point to Fermi level when the strain increase positively.

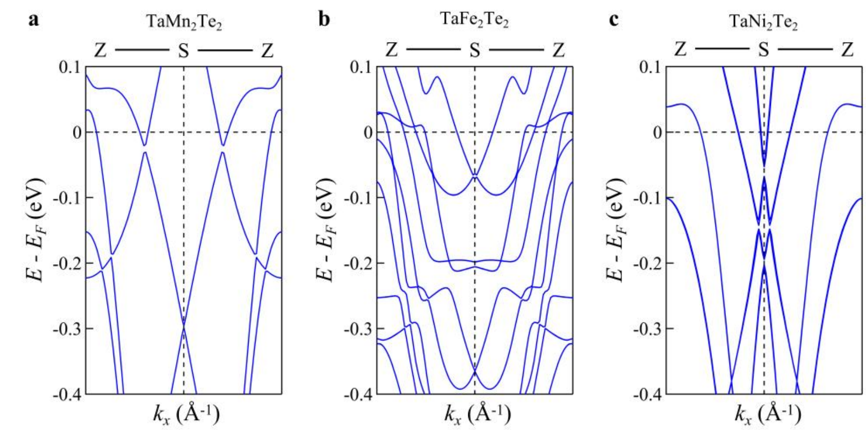

Supplementary Figure 5. The band structure of $TaMn_2Te_2$ (antiferromagnetism) (a), $TaFe_2Te_2$ (antiferromagnetism) (b) and $TaNi_2Te_2$ (non-magnetism) (c). Changing the magnetic atoms may not only change the magnetic ground state of the material, but also change the band dispersion near the Fermi level.

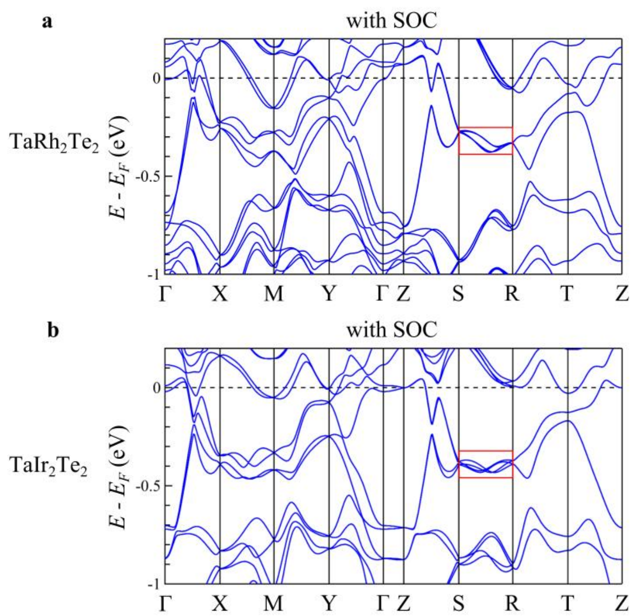

Supplementary Figure 6. DFT calculated dispersions along the high-symmetry path of $TaRh_2Te_2$ (a) and $TaIr_2Te_2$ (b) with considering SOC. The plotted band structures were calculated using the orthorhombic structural unit cell with lattice constants $a = 6.674\,Å$, $b = 6.860\,Å$, $c = 17.955\,Å$ for $TaRh_2Te_2$ and $a = 6.726\,Å$, $b = 6.844\,Å$, $c = 18.132\,Å$ for $TaIr_2Te_2$ in space group 62 ($Pmcn$). The hourglass fermion features are indicated by the red rectangle which are zoomed in Figure 3 (g) for $TaRh_2Te_2$ and (h) for $TaIr_2Te_2$ in the main text. The overall calculated band structures of $TaRh_2Te_2$ and $TaIr_2Te_2$ seem similar with $TaCo_2Te_2$, but there are differences in some details. Firstly, bands around Z along the $Z-S$ direction and $Z-T$ direction are both electron-like near the Fermi level and there is no VHS at Z point in $TaRh_2Te_2$ and $TaIr_2Te_2$. Secondly, SOC induced gap at the eightfold degenerate point (at S point) is larger

(~1.5 meV) for $TaIr_2Te_2$. Thirdly, due to the stronger SOC effect in $TaIr_2Te_2$, the hourglass fermion features are more visible.